

Computer Simulation of Crystal Structures Applied to the Solution of the Superstructure of Cubic Silcondiphosphate

E. TILLMANN AND W. GEBERT

Institut für Mineralogie, Ruhr-Universität, Bochum, Deutschland

AND

W. H. BAUR

Department of Geological Sciences, University of Illinois at Chicago, Chicago, Illinois 60680, and Institut für Kristallographie, Universität Karlsruhe, Karlsruhe, Deutschland

Received July 12, 1972

The superstructure of cubic SiP_2O_7 has a volume 27 times as large as the substructure of this compound. Because conventional methods failed in solving the superstructure, computer simulation of the structure was applied. Computer simulation depends on the accurate prediction of individual interatomic distances in a structure and on an appropriate weighting scheme. The predicted distances are treated as observations in a distance least-squares refinement, in which the positional coordinates of the atoms are varied until the calculated distances conform to the predicted values. Cubic SiP_2O_7 ($a = 22.418$ Å, space group $Pa\bar{3}$, $Z = 108$, $D_x = 3.22$) has 50 atoms in the asymmetric unit. The initial R -value for the simulated structure was 0.18, which dropped to 0.061 after three cycles of least squares refinement using $F_{\text{obsd}} = 1382$. In the substructure, all P-O-P angles in the diphosphate groups are straight because of symmetry requirements, and the angles P-O-Si are 164° . In the superstructure, the average angle P-O-P is 150° ; the average P-O-Si angle is 149° . The tendency to decrease these angles may be responsible for the formation of the superstructure. However, two diphosphate groups retain, even in the superstructure, the 180° configuration. Such a feature is usually only observed in high temperature polymorphs and is explainable as a positional disorder of bent P_2O_7 groups, or by the assumption of a highly anisotropic motion of the bridging oxygen atom. The silicon atoms in cubic SiP_2O_7 are octahedrally coordinated, as they are in the two monoclinic polymorphs of SiP_2O_7 . However, the three modifications are topologically distinct from each other as can be proved by considering the three-dimensional nets on which the three structures are based.

Introduction

It is presently not possible to calculate from first principles the details of an inorganic crystal structure, that is, the coordinates of its atomic positions and its unit cell parameters. Even the Born model, based on electrostatic interactions between ions, which can be of use in special applications such as the calculation of hydrogen atom positions in hydrogen containing compounds (1), seems to be of limited value as a general method of calculating crystal structures. The main problem with the Born model is that most compounds which can be treated as being ionic are so to a first approximation only,

and most likely the atoms in them carry only fractions of their formal charges [electroneutrality postulate (2)]. In order to avoid the problems inherent in the use and interpretation of different bonding models (ionic versus covalent), it has been proposed (3) to take a positivistic approach and to rely only on the crystal chemical information which is reasonably certain, namely on the interatomic distances. The distances between atoms in crystalline structures can be predicted with sufficient accuracy if one takes into consideration the coordination numbers of both anions and cations (4), the extended electrostatic valence rule (5, 6), and the effects of shared edges between

different coordination polyhedra (3). For a given trial structure of a given compound, a set of interatomic distances can be predicted and used as input into a distance least-squares refinement (DLS, (7)) as long as the number of predicted distances exceeds the number of parameters. In DLS the predicted interatomic distances are used as observations, and the positional parameters are adjusted in such a way that the calculated interatomic distances in the crystal structure correspond as closely as possible to the predicted distances. If the weights assigned to the predicted cation-anion distances are chosen proportional to the bond strengths of these distances, and the weights assigned to the anion-anion distances are taken to be small when compared with the weights given to the cation-anion distances, then the DLS refinement is similar to a simple force model, which takes account of the different strengths of the different bonds in a structure. The lengths of the bonds represent the lengths of elastic springs, the weights correspond to the restoring forces. If one chooses the predicted distances only within the coordination polyhedra, the method is equivalent to crystal structure model building using elastically flexible coordination polyhedra. Therefore it is proposed to call this method computer modeling or computer simulation of crystal structures.

The method has been applied so far to (a) the refinement of crystal structures which are well known from X ray diffraction studies in order to compare the simulated structures with the actual structures [framework silicates (7); olivine-type Mg_2SiO_4 (3)]; and a series of unpublished studies, Baur, 1971], (b) the refinement of a crystal structure for which only inaccurate powder diffraction data were available (8), (c) the refinement of a pseudosymmetric structure which could not be deduced directly from the X ray data [hydrated NaA (9)], (d) the refinement of hypothetical structures in order to compare them with the observed polymorphs of the same chemical composition [hypothetical Mg_2SiO_4 phases (3)], and (e) the refinement of crystal structures which cannot be studied by diffraction methods at the conditions under which they are stable [high pressure phases of Mg_2SiO_4 (3)].

In this paper we are applying computer modeling of a crystal structure to the solution of the superstructure of cubic SiP_2O_7 , a problem which could not be solved with more conventional methods. The diphosphates of Si, Ge, Sn, Pb, Ti, Zr, Hf, Ce, and U form a series of isostruc-

tural cubic crystals. Levi and Peyronel (10) determined from X ray powder diffraction data the structure of ZrP_2O_7 ($a=8.20$ Å, space group $Pa3$) and found SiP_2O_7 to be isostructural. The result of this structure determination was unusual in two respects: Zr (and therefore Si) have an octahedral six-coordination, and the angle around the bridging oxygen atom of the diphosphate group is 180° , since it is located in a center of symmetry. Völlenknecht *et al.* (11) showed, however, that Levi and Peyronel had apparently determined only a substructure. They found in single crystal X ray photographs of GeP_2O_7 superstructure reflections which tripled the unit cell edge of these compounds, thus increasing the cell volume 27 times. Hagman and Kierkegaard (12) prepared single crystals of ZrP_2O_7 and collected a complete set of three-dimensional single crystal diffraction data which included the superstructure reflections. However, they refined only the substructure and have not reported since any work on the superstructure. Liebau *et al.* (13) prepared single crystals of cubic SiP_2O_7 -AI and of two other closely related monoclinic polymorphs of SiP_2O_7 which they called SiP_2O_7 -AIII and SiP_2O_7 -AIV. The crystal structures of the monoclinic polymorphs were subsequently determined (14, 15).

Single crystals of cubic SiP_2O_7 , prepared by O. W. Flörke, were put at our disposal. We decided to attempt a solution of the superstructure of cubic SiP_2O_7 in order to clarify the relationship of cubic SiP_2O_7 to the monoclinic polymorphs of SiP_2O_7 , to resolve the question of the linear P-O-P bonds, and to study one further example of Si in octahedral coordination.

Experimental

Single crystals of cubic SiP_2O_7 were grown by transport reaction from material of the composition $Li_{0.25}Al_{0.25}Si_{0.75}P_2O_7$ in a platinum tube. The hot part of the tube with the sample was held at $1000^\circ C$ for three days, the colder part of the tube had a temperature of $960^\circ C$. The colorless crystals found in the colder part of the tube were nearly spherical in shape and showed a large number of different faces. A microprobe analysis of some of the crystals showed a ratio of $SiO_2:P_2O_5=1:0.99$. The crystals did not contain any aluminum. Table I gives crystal data and the details of data collection. The unit cell constant is based on the refinement of the setting of 12 reflections which had been centered

TABLE I
CRYSTAL DATA AND DETAILS OF DATA COLLECTION^a

	Substructure (S-structure)	Both	Superstructure (X-structure)
$a(\text{\AA})$	7.473(1)		22.418(2)
$V(\text{\AA}^3)$	417.3(3)		11267(3)
Z	4		108
FW		202.3	
$D_x(\text{g/cm}^3)$		3.22	
Space group		$Pa\bar{3}$	
Crystal diam (cm)		0.02	
$\mu(\text{MoK}\alpha)$ (cm^{-1})		13.0	
μR		0.13	
$2\theta_{\text{max}}(^{\circ})$		48	
Number of nonunique I_{hkl}		9824	
Number of unique I_{hkl}	108	2935	2827
Number of $I_{hkl} = 0$	8	1553	1545
Number of I_{hkl} used in refinement	100	1382	1282
Average relative intensity (zeros included)	28	5	4
Average relative intensity (zeros excluded)	30	11	9
$R_{(\text{substructure})}$	0.137		
$R_{(\text{superstructure})}$	0.031	0.061	0.069
$wR_{(\text{superstructure})}$	0.046	0.066	0.071

^a Throughout this paper, the number in parentheses, following a numerical value, indicates the estimated standard deviation in units of the least significant digit.

on an automatic 4-circle X ray diffractometer. Systematic extinctions ($Ok\bar{l}$ present only with $k = 2n$) led to space group $Pa\bar{3}$.

Intensity data were collected on an automatic 4-circle X ray diffractometer using Zr-filtered $\text{MoK}\alpha$ radiation ($\lambda = 0.7107 \text{ \AA}$), θ - 2θ step-scan mode with 50 steps of 0.01° , 1 sec counting time per step and 5 sec background counting time. A list of computer programs used in the course of the work is given by Baur and Khan (16). In addition, the Fourier program, SFS, by Neukäter and Biedl (unpublished) and the program DLS (distance least-squares) by Meier and Villiger (7) were used. The measured intensities were corrected for Lorentz-polarization effects, and the individual values of the squared structure amplitudes and their standard deviations were averaged for equivalent reflections. Since the crystal used for data collection was almost spherical in shape and the value of μR was small, an absorption correction was not necessary. The calculation of standard deviations $\sigma(I)$ is described by Corfield, Doedens, and Ibers (17). Any intensity measured to be less than two

times its standard deviation was considered to be zero.

Solution of the Structure

The atomic coordinates given by Levi and Peyronel (10) for the substructure of the isomorphous compound ZrP_2O_7 were used as starting parameters for a least-squares refinement of the substructure of SiP_2O_7 . Only those reflections were used in the refinement which had indices in the form $h = 3n$, $k = 3n$ and $l = 3n$, when referred to the supercell. Atomic scattering factors were taken from the International Tables for X ray Crystallography (18). The function minimized was $\sum w(|F_o| - |F_c|)^2$, with F_o and F_c being the observed and calculated structure amplitudes. The weight w was defined as $(1/\sigma^2)F_o$. The refinement converged after 3 cycles at an R -value of 0.137. The results are given in Table II.

As could be expected, the P-O and Si-O distances in the substructure, in which three of the four crystallographically different atoms lie in special positions, are appreciably shorter than

TABLE II

REFINEMENT OF THE SUBSTRUCTURE OF SiP_2O_7

1. Positional and thermal parameters with estimated standard deviations. The x , y , z are fractions of the cell edge, B is in \AA^2 .

	Position	$x(\sigma)$	$y(\sigma)$	$z(\sigma)$	$B(\sigma)$
Si	4(a)	0.0	0.0	0.0	1.8(2)
P	8(c)	0.3833(5)	0.3833(5)	0.3833(5)	1.4(1)
O(1)	4(b)	0.5	0.5	0.5	10(2)
O(2)	24(d)	0.441(2)	0.202(2)	0.408(2)	5.8(4)

2. Interatomic distances and angles.

	Distance (\AA)	Angle ($^\circ$)
Si-O(2)(6 \times)	1.72(2)	
O(2)-O(2)(6 \times)	2.40(2)	O(2)-Si-O(2)(6 \times) 89(1)
O(2)-O(2)(6 \times)	2.45(2)	O(2)-Si-O(2)(6 \times) 91(1)
O(2)-O(2)(3 \times)	3.43(2)	O(2)-Si-O(2)(3 \times) 180(1)
P-O(1)	1.51(2)	P-O(1)-P 180(1)
P-O(2)(3 \times)	1.43(1)	P-O(2)-Si 164(1)
O(2)-O(2)(3 \times)	2.37(2)	O(2)-P-O(2)(3 \times) 112(1)
O(1)-O(2)(3 \times)	2.37(2)	O(2)-P-O(1)(3 \times) 107(1)

they should be when compared with accepted values. The fact that the substructure is an average structure is also characterized by the high isotropic temperature factors of all atoms. Since the temperature factors of the oxygen atoms were relatively higher than those of the metal atoms, differences in atomic positions between substructure and superstructure were expected to be larger for the oxygen atoms.

The Fourier synthesis of the substructure corresponds to an averaging of the 27 subcells of the supercell. Every peak in the subcell, therefore, is a superposition of 27 different atomic positions of the superstructure. The unraveling of these 27 positions and their correct assignment to one of the 27 subcells is an impossible task. This situation differs sharply from the problem faced by Katz and Megaw (19) in their solution of the pseudosymmetric structure of KNbO_3 , where every superposed atom had to be split into two half-atoms. We attempted this approach, nevertheless, hoping that some of the asymmetries in the shapes of the oxygen atoms of the substructure could be interpreted as atomic positions in the superstructure. None of the trial models succeeded, however. The R -values remained at about 0.60 and the least-squares

refinements diverged as was apparent from the chemically impossible interatomic distances resulting from these refinements. As has been pointed out by Katz and Megaw (19), a direct automatic refinement cannot be started from an average structure because the assumption that the structure factors vary linearly with the atomic coordinates "throughout the range examined, is certainly not valid when the range includes special values". Direct methods of phase determination were not tried. The signs of the strong reflections (from the substructure) were known already, and the chances of determining the phases of the superstructure reflections were considered to be extremely small. Computer modeling, however, appeared to be applicable: a trial structure was available since the topology of the superstructure is known from the substructure. The predicted input distances (Table III) were based on the following reasoning. The P-O distances to the terminal (O_T) and the bridging (O_B) oxygen atoms of the P_2O_7 group should be 1.51 and 1.57 \AA based on Shannon and Prewitt's (4) radii and on the extended electrostatic valence rule (5). In SiP_2O_7 -AIII and SiP_2O_7 -AIV, average distances of 1.49 and 1.59 \AA have been observed for P- O_T and P- O_B , respectively.

TABLE III

PREDICTED INTERATOMIC DISTANCES AND CORRESPONDING WEIGHTS USED AS INPUT INTO THE DLS-REFINEMENT

	Distance (Å)	Weight
Si-O	1.76	0.67
(O-O) _{octahedral}	2.49	0.30
P-O _B	1.58	1.25
P-O _T	1.50	1.25
(O _T -O _T) _{tetrahedral}	2.50	0.30
(O _B -O _T) _{tetrahedral}	2.46	0.30
P-O _B ^a	1.54	1.00
(O _B -O _T) _{tetrahedral} ^a	2.43	0.30

^a Distances involving oxygen atoms O(5) and O(6) in special positions.

We chose as input the means of these calculated and observed distances. For the P₂O₇-groups with the bridging oxygen atoms in a special position [O(5) and O(6)], P-O_B was chosen to be 1.54 Å in accord with the value observed in β-Cu₂P₂O₇ (20) where the angle P-O-P is also 180°. The distances O_B-O_T and O_T-O_T in the tetrahedra were chosen to differ slightly from each other because of the observations made on condensed phosphates (5). The distance Si-O was taken from rutile-type SiO₂ (21) and corrected for the different coordination numbers of the oxygen atoms in these two compounds. The distance O-O in the SiO₆ octahedron was calculated assuming an angle O-Si-O of 90°. The weights assigned to the Si-O and P-O distances were based on the electrostatic bond strengths of these bonds. The weight for P-O_B was reduced slightly because of the greater uncertainty involving this bond length. The O-O distances were uniformly given weights of 0.30 which is higher than the weights assigned to the polyhedral edges in the simulation of the Mg₂SiO₄ polymorphs (3) because we wanted the polyhedra to remain relatively rigid. A total of 173 crystallographically different distances was predicted in this way, while only 134 positional coordinates had to be determined.

The function minimized in the DLS-refinement was $\sum_j \sum_{m,n} [w^{(j)}(D_{m,n}^{(j)} - BL^{(j)})]^2$, where $BL^{(j)}$ is the predicted interatomic distance, $D_{m,n}^{(j)}$ the actual distance between atoms m and n , $w^{(j)}$ the weight assigned to this interatomic distance. Nine cycles of DLS refinement gave a chemically reasonable model of the structure

(D-structure). In this case, only interatomic distances within each coordination polyhedron had been predicted, but distances between atoms in different polyhedra also had the expected values. A structure factor calculation for the D-structure showed an R -value of 0.181, a new least-squares refinement with the observed structure amplitudes as observations converged after three cycles, in which 185 parameters were varied, at R equal to 0.061.

The values of $|F_0|$ and F_c for the X-structure are listed in Table IV, the 1553 unobserved reflections are not included. The high R -value of 0.308 for all 2935 reflections is caused by the fact that more than 50% of the reflections are unobserved ($F_0 = 0$); all calculated structure amplitudes for unobserved reflections, however, are of a magnitude comparable to the weakest observed structure amplitude. The final positional and thermal parameters of the superstructure (X-structure) and the positional parameters of the substructure (S-structure) and the D-structure are listed in Table V. Table VI gives the mean differences between atomic positions and between interatomic distances in the three structures.

Description and Discussion of the Crystal Structure

All silicon atoms in cubic SiP₂O₇ are octahedrally six-coordinated; all phosphorus atoms are tetrahedrally coordinated by oxygen atoms. The phosphate tetrahedra share one of their vertices with a second tetrahedron, thus forming diphosphate groups [P₂O₇]⁻⁴. All the oxygen atoms are two-coordinated: they are bonded either to two phosphorus atoms or to one phosphorus and one silicon atom each. The Si atoms are arranged approximately face centered (relative to the subcell) and so are the bridging oxygen atoms of the P₂O₇ groups: the Si atoms and the bridging oxygen atoms are in positions corresponding to the Na and Cl positions in the NaCl-type structure. Every unit cell of the superstructure contains 27 such NaCl-type cells. From this description it is obvious that every diphosphate group is surrounded by six different octahedral groups, while every octahedral group is surrounded by six diphosphate groups. The terminal oxygen atoms of a staggered diphosphate group are similarly arranged as in an octahedral group which is elongated along one of its three-fold axes. Therefore, we can view the cubic SiP₂O₇ structure also as a distorted

TABLE IV
OBSERVED AND CALCULATED STRUCTURE FACTORS (x0.3)

Table with multiple columns of numerical data representing structure factors. The columns are organized in groups of four, with headers like 'h k l' and 'FO FC'. The data is presented in a grid format, showing observed (FO) and calculated (FC) values for various hkl reflections.

TABLE V

POSITIONAL AND THERMAL PARAMETERS OF THE X-STRUCTURE, AND POSITIONAL PARAMETERS OF THE S-STRUCTURE AND THE D-STRUCTURE

Position		X-structure				D-structure			S-structure		
		x(G)	y(G)	z(G)	B(Å)	x	y	z	x	y	z
P(1)	24(d)	0.4619(2)	0.1211(2)	0.1292(2)	0.3(1)	0.4633	0.1191	0.1272	0.4610	0.1277	0.1277
P(2)	"	0.4759(2)	0.4528(2)	0.1281(2)	0.4(1)	0.4799	0.4515	0.1280	0.4610	0.4610	0.1277
P(3)	"	0.7859(2)	0.1230(2)	0.1354(2)	0.3(1)	0.7851	0.1202	0.1373	0.7943	0.1277	0.1277
P(4)	"	0.7965(2)	0.7910(2)	0.1337(2)	0.4(1)	0.7969	0.7896	0.1354	0.7943	0.7943	0.1277
P(5)	"	0.1259(2)	0.4728(2)	0.7965(2)	0.3(1)	0.1247	0.4747	0.7986	0.1277	0.4610	0.7943
P(6)	"	0.1280(2)	0.7851(2)	0.4604(2)	0.5(1)	0.1264	0.7828	0.4600	0.1277	0.7943	0.4610
P(7)	"	0.4618(2)	0.7883(2)	0.4653(2)	0.4(1)	0.4609	0.7853	0.4663	0.4610	0.7943	0.4610
P(8)	"	0.4709(2)	0.8010(2)	0.7834(2)	0.3(1)	0.4742	0.8027	0.7836	0.4610	0.7943	0.7943
P(9)	8(c)	0.7997(2)	0.7997(2)	0.7997(2)	0.3(1)	0.8005	0.8005	0.8005	0.7943	0.7943	0.7943
P(10)	"	0.4602(2)	0.4602(2)	0.4602(2)	0.2(1)	0.4603	0.4603	0.4603	0.4610	0.4610	0.4610
P(11)	"	0.1196(2)	0.1196(2)	0.1196(2)	0.3(1)	0.1202	0.1202	0.1202	0.1277	0.1277	0.1277
Si(1)	24(d)	0.3372(2)	-0.0019(2)	-0.0054(2)	0.5(1)	0.3397	-0.0015	-0.0056	0.3333	0.0	0.0
Si(2)	"	0.3221(2)	0.3393(2)	-0.0032(2)	0.6(1)	0.3197	0.3412	-0.0046	0.3333	0.3333	0.0
Si(3)	"	-0.0080(2)	0.3355(2)	0.6519(2)	0.4(1)	-0.0093	0.3351	0.6506	0.0	0.3333	0.6667
Si(4)	"	0.3432(2)	0.6612(2)	0.3293(2)	0.4(1)	0.3462	0.6595	0.3298	0.3333	0.6667	0.3333
Si(5)	8(c)	0.3340(2)	0.3340(2)	0.3340(2)	0.7(2)	0.3338	0.3338	0.3338	0.3333	0.3333	0.3333
Si(6)	4(a)	0.0	0.0	0.0	0.4(2)	0.0	0.0	0.0	0.0	0.0	0.0
O(1)	24(d)	0.4930(4)	0.1454(4)	0.1886(4)	0.0(2)	0.4941	0.1420	0.1864	0.5000	0.1666	0.1666
O(2)	"	0.8130(4)	0.1720(4)	0.1714(5)	0.6(2)	0.8121	0.1743	0.1734	0.8333	0.1667	0.1667
O(3)	"	0.5107(4)	0.4786(4)	0.1829(4)	1.0(2)	0.5114	0.4795	0.1845	0.5000	0.5000	0.1667
O(4)	"	0.1852(5)	0.4997(4)	0.8221(4)	0.7(2)	0.1848	0.4992	0.8263	0.1667	0.5000	0.8333
O(5)	8(c)	0.1592(5)	0.1592(5)	0.1592(5)	2.0(5)	0.1598	0.1598	0.1598	0.1667	0.1667	0.1667
O(6)	4(b)	0.5000	0.5000	0.5000	1.1(5)	0.5000	0.5000	0.5000	0.5000	0.5000	0.5000
O(7)	24(d)	0.1167(5)	0.0591(4)	0.1476(4)	0.9(2)	0.1181	0.0600	0.1491	0.1470	0.0670	0.1360
O(8)	"	0.4867(4)	0.0597(4)	0.1196(4)	0.5(2)	0.4876	0.0578	0.1155	0.4800	0.0670	0.1360
O(9)	"	0.1425(5)	0.3952(4)	0.1171(4)	0.4(2)	0.1405	0.3977	0.1190	0.1470	0.4010	0.1360
O(10)	"	0.1627(4)	0.0799(4)	0.4787(4)	0.5(2)	0.1618	0.0790	0.4814	0.1470	0.0670	0.4690
O(11)	"	0.4996(4)	0.3901(4)	0.1203(4)	0.5(2)	0.5015	0.3886	0.1210	0.4800	0.4010	0.1360
O(12)	"	0.4937(4)	0.0765(4)	0.4920(5)	0.6(2)	0.4935	0.0779	0.4942	0.4800	0.0670	0.4690
O(13)	"	0.1408(4)	0.4106(4)	0.4520(5)	0.8(2)	0.1426	0.4147	0.4537	0.1470	0.4010	0.4690
O(14)	"	0.4537(4)	0.4021(4)	0.4923(4)	0.6(2)	0.4498	0.4040	0.4949	0.4800	0.4010	0.4690
O(15)	"	0.8075(4)	0.0655(4)	0.1629(4)	0.7(2)	0.8078	0.0649	0.1673	0.8140	0.0670	0.1360
O(16)	"	0.1418(5)	0.7190(5)	0.1272(4)	0.7(2)	0.1446	0.7188	0.1241	0.1470	0.7340	0.1360
O(17)	"	0.1274(5)	0.0719(5)	0.8058(4)	0.8(2)	0.1254	0.0740	0.8059	0.1470	0.0670	0.8030
O(18)	"	0.8185(5)	0.7293(5)	0.1386(5)	1.0(2)	0.8200	0.7270	0.1397	0.8140	0.7340	0.1360
O(19)	"	0.8162(4)	0.0769(4)	0.8185(4)	0.6(2)	0.8183	0.0790	0.8185	0.8140	0.0670	0.8030
O(20)	"	0.1420(5)	0.7289(5)	0.7946(5)	0.7(2)	0.1427	0.7307	0.7957	0.1470	0.7340	0.8030
O(21)	"	0.8217(4)	0.7361(4)	0.8041(4)	0.5(2)	0.8219	0.7379	0.8107	0.8140	0.7340	0.8030
O(22)	"	0.1326(5)	0.4063(5)	0.7946(5)	0.7(2)	0.1297	0.4079	0.7975	0.1470	0.4010	0.8030
O(23)	"	0.1436(4)	0.7195(5)	0.4582(5)	0.5(2)	0.1440	0.7183	0.4594	0.1470	0.7340	0.4690
O(24)	"	0.5020(4)	0.7362(4)	0.1187(4)	0.5(2)	0.5035	0.7382	0.1224	0.4800	0.7340	0.1360
O(25)	"	0.4630(4)	0.7254(4)	0.4897(4)	0.7(2)	0.4600	0.7240	0.4931	0.4800	0.7340	0.4690
O(26)	"	0.4889(4)	0.4086(4)	0.8217(4)	0.7(2)	0.4862	0.4091	0.8228	0.4800	0.4010	0.8030
O(27)	"	0.5048(4)	0.7457(4)	0.7997(4)	0.6(2)	0.5091	0.7488	0.8025	0.4800	0.7340	0.8030
O(28)	"	0.4923(4)	0.0692(4)	0.7933(4)	0.3(2)	0.4907	0.0680	0.7934	0.4800	0.0670	0.8030
O(29)	"	0.8364(4)	0.0753(4)	0.4924(4)	0.6(2)	0.8404	0.0763	0.4942	0.8140	0.0670	0.4690
O(30)	"	0.8121(5)	0.3991(4)	0.1279(5)	0.7(2)	0.8105	0.3992	0.1295	0.8140	0.4010	0.1360
O(31)	"	0.7875(4)	0.3976(4)	0.4659(4)	0.4(2)	0.7831	0.3998	0.4677	0.8140	0.4010	0.4690
O(32)	"	0.8062(5)	0.4065(5)	0.8003(5)	0.6(2)	0.8067	0.4114	0.8039	0.8140	0.4010	0.8030
O(33)	"	0.8125(4)	0.7175(5)	0.4702(5)	0.6(2)	0.8130	0.7174	0.4749	0.8140	0.7340	0.4690

ReO₃-type in which alternately every other octahedron is replaced by a staggered ditetrahedral group. This changes, of course, the stoichiometry because the two cations and the bridging oxygen atom of the ditetrahedral group have to replace one cation in octahedral coordination.

An alternate way of describing this structure is to view it as a three-dimensional net consisting of four-connected points (P atoms) and six-connected points (Si atoms). In this description the oxygen atoms can be ignored because they are only two-connected points and can be taken to be the connectors between the Si and P atoms

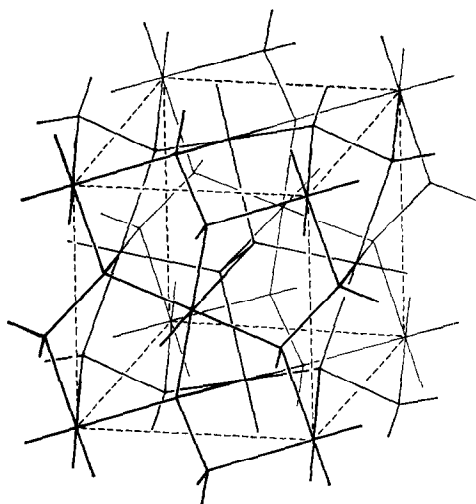


FIG. 1. Representation of the substructure of cubic SiP_2O_7 as a (4,6) connected three-dimensional net. One unit cell (dashed) and its immediate surroundings are shown.

(Fig. 1). Starting from any 4- or 6-connected point in this net, it is possible to return to the original point by going through a shortest complete circuit consisting of only 5 points: $-\text{P}_a-\text{Si}_a-\text{P}_b-\text{P}_c-\text{Si}_b-\text{P}_a-$. Since all these puckered 5-gons are topologically equivalent we can call this net a uniform (4,6) net, with the symbol $(5^6)_2(5^{12})$, which means: there are twice as many four-connected points as there are six-connected points (see the subscript), also at every four-connected point six 5-gons have a common vertex, while at every six connected point 12 5-gons have a common vertex (see the superscript). The symbol is analogous to the ones used by Wells in his papers on the geometrical basis of crystal chemistry (particularly Ref. 22). His approach is useful for distinguishing topologically distinct nets. If two different crystal structures can be shown to be based on nets having different symbols, they must be topologically distinct. Unfortunately, the reverse is not true: two topologically distinct nets could still have the same symbol. An investigation of SiP_2O_7 -AIII shows it to be based on a (4,6) net with the symbol $(4^3.5^2.6)_2(4^4.5^4.6^4)$, while SiP_2O_7 -AIV can be reduced to a (4,6) net with the symbol $(4.5^4.6)^2(4^4.5^4.6^4)$. From this, it is obvious that the monoclinic polymorphs cannot be lower symmetry distortions of cubic SiP_2O_7 but are distinct polymorphs which could be formed from

cubic SiP_2O_7 only through a reconstructive transformation. While both SiP_2O_7 -AIII and SiP_2O_7 -AIV are based on nets containing shortest circuits consisting of 4, 5 and 6 four- or six-connected points, they still are different from each other as can be seen from the surrounding of the four-connected points: in SiP_2O_7 -AIII, three 4-gons are meeting at the tetrahedral point; in SiP_2O_7 -AIV there is only one 4-gon adjacent to the 4-connected point. Furthermore, in SiP_2O_7 -AIV, some of the 6-gons are of the type $-\text{P}_a-\text{Si}_a-\text{P}_b-\text{Si}_b-\text{P}_c-\text{Si}_c-\text{P}_a-$ with alternating 4- and 6-connected points, while, in SiP_2O_7 -AIII, all 6-gons are of the type $-\text{P}_a-\text{P}_b-\text{Si}_a-\text{P}_c-\text{P}_a-\text{Si}_b-\text{P}_a-$.

In the superstructure, only two atoms are located exactly at the same positions in which they are situated in the substructure: O(6) and Si(6), which are in the supercell in $1/2, 1/2, 1/2$ and 000. All other atoms have moved from their substructure positions (Fig. 2). The mean displacement of the atoms is 0.40 Å, whereby the oxygen atoms have moved on the average 0.48 Å (ranging from 0.16 to 0.79 Å), while the P and Si atoms have moved on the average 0.23 Å (ranging from 0.03 to 0.38 Å). No less than 16 or almost one half of the oxygen atoms have been displaced by one-half Ångström or more out of their positions in the averaged structure. The displacements are such that the angle P-O-P which is 180° in the substructure now ranges from 144 to 149° (except for the diphosphate groups in special positions), while the angle P-O-Si, which is 164° in the substructure, is assuming values from 137 to 173° (mean 149°) in the super-

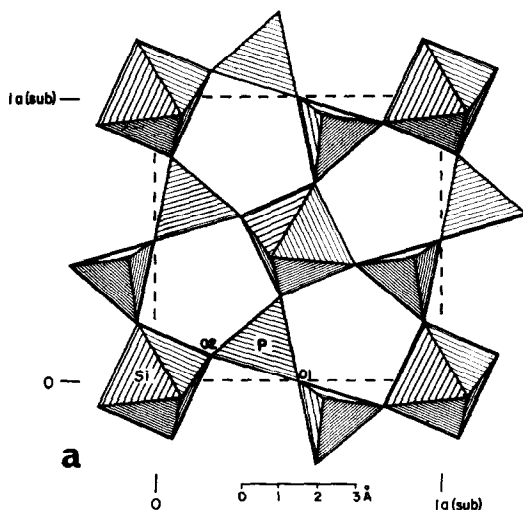


FIG. 2a.

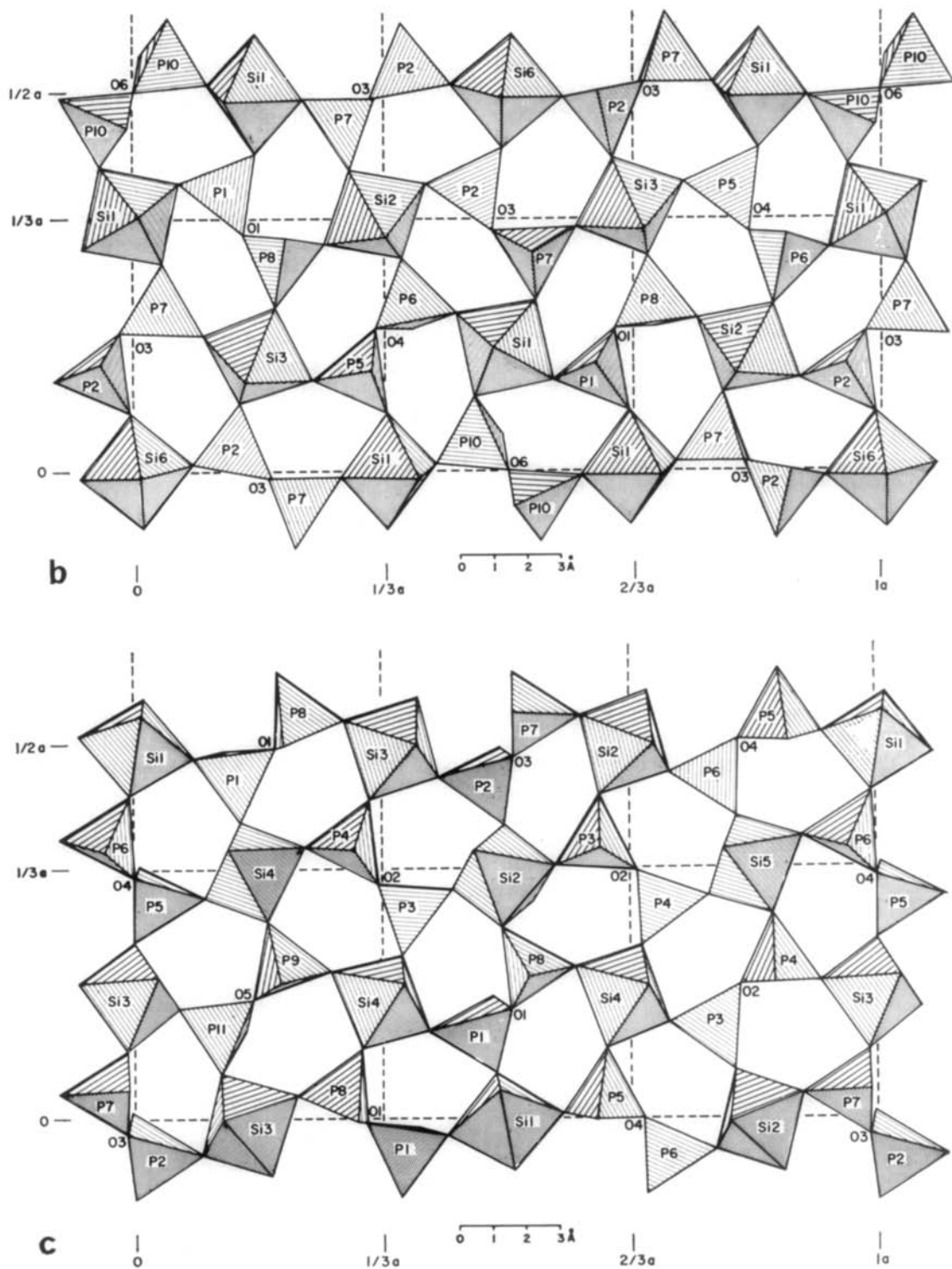


FIG. 2. (a) Polyhedral representation of one layer (close to x equal zero) of substructure of cubic SiP_2O_7 . (b) The same for superstructure of cubic SiP_2O_7 . (c) Layer of cubic SiP_2O_7 close to x equal $1/6$. In the case of (b) and (c), one half of the unit cell is presented. The deviations of the superstructure from the average structure are clearly visible.

structure. It appears, therefore, that the superstructure allows values of the P–O–Si and P–O–P angles which are more in line with those observed in $\text{SiP}_2\text{O}_7\text{-AIII}$, $\text{SiP}_2\text{O}_7\text{-AIV}$, and other comparable structures, while this would not be possible in the substructure.

The D-structure and the refined X ray structure are very similar, which is apparent from the initial *R*-value of 0.18. One way to compare the D-structure with the X-structure is to look at the differences in the P–O, Si–O and O–O distances within the coordination polyhedra between the two refinements: this difference is on the average 0.023 Å (Table VI). The corresponding average difference in the P–P and P–Si distances which are about 3.1 Å in length (which means removed from each other by one bridging oxygen atom) is 0.022 Å. If we compare, however, the distances of every atom in the D-structure to the corresponding atom in the X-structure, we find their average distance to be 0.075 Å. This means that the simulated D-structure has reproduced very accurately the shapes and dimensions of the coordination polyhedra and their relative positions in the immediate vicinity of each polyhedron. The average deviation of 0.023 Å has to be judged on the basis of the estimated standard deviations of the bond length in the X-structures which range from 0.006 Å for P–P and P–Si to 0.014 Å for the O–O distances. On the other hand, the average distance of 0.075 Å from D-atom to X-atom tells us that the positioning of the polyhedra within the unit cell and, therefore, the relative positions of further removed

polyhedra from each other are not reproduced quite that precisely by the D-structure. This is not surprising since it shows us that the interatomic distances which have not been predicted and used as input into the DLS-refinement are not simulated as well as those which were used as DLS-input. This points to the possibility of improving the simulation procedure by entering into the model nonbonded interactions. One could include, for instance, van der Waals forces between oxygen atoms belonging to different polyhedra, analogous to the potential calculations on molecular structures (23).

The configuration of the P_2O_7 groups in the substructure is staggered, which means that the two triangles outlined by the terminal oxygen atoms at opposite ends of the diphosphate group are rotated by 180° relative to each other. In the superstructure only the diphosphate group around O(6) is required by symmetry to have a staggered configuration. The groups around O(1) and O(4) actually are very close to a staggered configuration, while the groups around O(2) and O(3) are in between a staggered and an eclipsed configuration, similar to the geometry of the P_2O_7 group in $\text{SiP}_2\text{O}_7\text{-AIV}$. The diphosphate group around O(5) can be called an almost eclipsed configuration, which is remarkable in view of the staggered configuration required by the substructure. This illustrates how severe the distortions of the superstructure are (Fig. 3), when compared with the substructure, which can be viewed as the idealized structure of cubic SiP_2O_7 . The angles P–O–P vary for the

TABLE VI
MEAN DIFFERENCES BETWEEN THE X-STRUCTURE AND THE D- AND S-STRUCTURES OF
CUBIC SiP_2O_7 ^a

	$\Delta(\text{Å})$	Range of Δ 's (Å)
Mean $\Delta(\text{X}, \text{S})$ for $(x, y, z)_{\text{P}, \text{Si}}$	0.235	0.026–0.383
Mean $\Delta(\text{X}, \text{S})$ for $(x, y, z)_{\text{O}}$	0.481	0.157–0.787
Mean $\Delta(\text{X}, \text{S})$ for $(x, y, z)_{\text{P}, \text{Si}, \text{O}}$	0.400	0.026–0.787
Mean $\Delta(\text{X}, \text{D})$ for $(x, y, z)_{\text{P}, \text{Si}}$	0.058	0.003–0.093
Mean $\Delta(\text{X}, \text{D})$ for $(x, y, z)_{\text{O}}$	0.084	0.023–0.154
Mean $\Delta(\text{X}, \text{D})$ for $(x, y, z)_{\text{P}, \text{Si}, \text{O}}$	0.075	0.003–0.154
Mean $\Delta(\text{X}, \text{D})$ for P–O and Si–O	0.013	0.000–0.056
Mean $\Delta(\text{X}, \text{D})$ for O–O in edges	0.028	0.000–0.120
Mean $\Delta(\text{X}, \text{D})$ for P–O, Si–O, and O–O	0.023	0.000–0.120
Mean $\Delta(\text{X}, \text{D})$ for P–P and P–Si	0.022	0.000–0.059

^a The ranges do not include the values involving atoms O(6) and Si(6), which are fixed by symmetry.

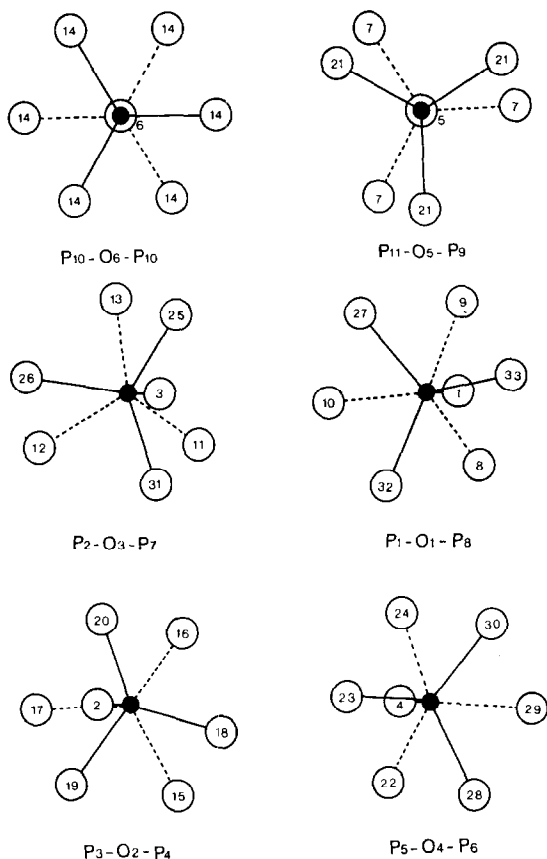


FIG. 3. Views of the diphosphate groups projected along the P-P vectors.

groups in general positions in the small range from 143.5 to 148.7° , which is distinctly and significantly higher than in $\text{SiP}_2\text{O}_7\text{-AIII}$ (139.2°) and $\text{SiP}_2\text{O}_7\text{-AIV}$ (132.4°). The diphosphate groups centered around O(5) and O(6) have straight P-O-P angles. The isotropic temperature factors for these two oxygen atoms are the highest of all the atoms in cubic SiP_2O_7 , even though the difference to the average isotropic temperature factors of all atoms is not significant for O(6) and only possibly significant for O(5). The quality of the diffraction data and the prohibitive cost of refining 405 positional, scale, and temperature parameters, unfortunately, did not allow an anisotropic temperature factor refinement. However, the fact that the temperature factors of O(5) and O(6) have by far the highest estimated standard deviations of all the atoms associated with them, points to the possibility that the thermal movement of these two atoms is highly anisotropic. This would be in accord with the observation made on the high-temperature form of

copper diphosphate (20). In $\beta\text{-Cu}_2\text{P}_2\text{O}_7$ (and in other isostructural thortveitite type β -phases), the major component of the thermal movement of the bridging oxygen atom is normal to the straight P-O-P linkage. This can be interpreted either as disorder of bent diphosphate groups or as real anisotropic movement. The question of whether the anisotropic thermal ellipsoid of the bridging oxygen atom in $\beta\text{-Cu}_2\text{P}_2\text{O}_7$ represents a space or a time average could not be decided by Robertson and Calvo (20). We have even less information to go by in cubic SiP_2O_7 , and, therefore, we must leave this question open.

The dimensions of the diphosphate groups agree with well established values known from other structure determinations (Table VII). The average values for all P-O_T and P-O_B bond lengths (Table VIII) agree well with the values predicted from the ionic radii and the extended electrostatic valence rule, which are 1.51 \AA for P-O_T and 1.57 \AA for P-O_B [with $p_{\text{O}_T} = 1.92$ v.u. (valence units) and $p_{\text{O}_B} = 2.50$ v.u., see (5)]. The observed average tetrahedral edge lengths for O_T-O_T and O_B-O_T are almost identical (Table VIII). Therefore, the difference in the observed mean tetrahedral angles O_T-P-O_T and O_B-P-O_T (111.5° and 107.3°) must be due to the displacement of the P-atoms within the oxygen atom tetrahedron towards the sides which display the larger tetrahedral angles, that is towards the O_T atoms. The same observation has been made previously for a number of orthophosphates (16). The relationship between bond angle and bond lengths can be expressed (5) as a linear relation:

$$\log[\sin(\bar{\alpha}/2)] = a + b \log(\overline{\text{P-O}})$$

where $\bar{\alpha}$ is the average over the three O_T-P-O_T or the three O_B-P-O_T angles in a tetrahedron, $\overline{\text{P-O}}$ is the corresponding average bond length of the sides of these angles, and a and b are the intercept and the slope of the regression equation. The correlation between bond angle and bond lengths is strong (Table IX) since 76% of the variation in bond angle can be explained by the dependence on the bond length. The slope and intercept found here for the SiP_2O_7 polymorphs are identical to the values found previously for orthophosphates.

The dimensions of the SiO₆ octahedra (Tables VIII and X) resemble most closely those found in $\text{SiP}_2\text{O}_7\text{-AIV}$, where the average Si-O bond length is 1.763 \AA . However, the average Si-O bond length

TABLE VII
 INTERATOMIC DISTANCES AND BOND ANGLES IN DIPHOSPHATE GROUPS^a

	Distance (Å)		Bond angle (°)		Distance (Å)	Bond angle (°)	Distance (Å)	Bond angle (°)
	O(10)	O(8)	O(10)	O(8)				
P(1)	1.493	1.499	112.0	112.0	1.492	110.9	2.474	110.9
	O(8)	O(9)	115.3	115.3	1.512	112.5	2.506	112.5
	O(9)	O(1)	107.1	107.1	1.521	110.2	2.507	110.2
	O(1)	O(8)	109.6	109.6	1.564	112.9	2.528	112.9
	O _T (m3)	O(8)	105.7	105.7	1.508	105.1	2.442	105.1
	O(m4)	O(9)	106.5	106.5	1.522	104.9	2.446	104.9
	Si(m3)	O _T , O _T (m3)	112.3	112.3	3.090	112.1	2.503	112.1
		O _B , O _T (m3)	106.4	106.4		106.7	2.465	106.7
P(3)	1.495	1.499	110.5	110.5	1.474	108.1	2.390	108.1
	O(15)	O(17), O(16)	112.5	112.5	1.478	111.8	2.486	111.8
	O(16)	O(17), O(2)	108.9	108.9	1.528	108.6	2.480	108.6
	O(2)	O(15), O(16)	109.4	109.4	1.578	114.5	2.529	114.5
	O _T (m3)	O(15), O(2)	108.9	108.9	1.493	108.8	2.487	108.8
	O(m4)	O(16), O(2)	106.6	106.6	1.514	104.7	2.460	104.7
	Si(m3)	O _T , O _T (m3)	110.8	110.8	3.194	111.5	2.468	111.5
		O _B , O _T (m3)	108.1	108.1		107.4	2.476	107.4
P(5)	1.499	1.509	112.5	112.5	1.503	112.5	2.507	112.5
	O(29)	O(22), O(24)	114.6	114.6	1.512	111.3	2.489	111.3
	O(24)	O(22), O(4)	107.9	107.9	1.513	110.4	2.532	110.4
	O(4)	O(29), O(24)	108.9	108.9	1.580	109.6	2.472	109.6
	O _T (m3)	O(29), O(4)	108.0	108.0	1.509	107.3	2.492	107.3
	O(m4)	O(24), O(4)	104.5	104.5	1.527	105.4	2.460	105.4
	Si(m3)	O _T , O _T (m3)	112.0	112.0	3.132	111.1	2.489	111.1
		O _B , O _T (m3)	106.8	106.8		107.7	2.495	107.7
P(7)	1.505	1.513	110.6	110.6	1.500	112.7	2.498	112.7
	O(31)	O(26), O(31)	113.8	113.8	1.500	112.8	2.525	112.8
	O(3)	O(26), O(3)	110.3	110.3	1.531	105.8	2.456	105.8
	O _T (m3)	O(25), O(31)	110.5	110.5	1.578	108.7	2.463	108.7
	O(m4)	O(25), O(3)	104.1	104.1	1.510	105.4	2.450	105.4
	Si(m3)	O(31), O(3)	107.1	107.1	1.527	111.1	2.564	111.1
		O _T , O _T (m3)	111.6	111.6	3.145	111.4	2.495	111.4
		O _B , O _T (m3)	107.2	107.2		107.4	2.490	107.4

							Distance (Å)	Bond angle (°)
P(9)	O(21) (3×)	1.510	O(21), O(21) (3×)	2.480	110.3	P(1)-O(1)-P(8)	3.026	144.4
	O(5)	1.596	O(21), O(5) (3×)	2.523	108.6	P(3)-O(2)-P(4)	3.037	148.7
	O(m4)	1.532				P(2)-O(3)-P(7)	2.985	143.5
	Si(3×)	3.180				P(5)-O(4)-P(6)	3.015	146.5
P(10)	O(14) (3×)	1.495	O(14), O(14) (3×)	2.484	112.4	P(9)-O(5)-P(11)	3.134	180.0
	O(6)	1.544	O(14), O(6) (3×)	2.434	106.4	P(10)-O(6)-P(10)	3.087	180.0
	O(m4)	1.507						
	Si(3×)	3.012						
P(11)	O(7) (3×)	1.496	O(7), O(7) (3×)	2.465	111.0			
	O(5)	1.538	O(7), O(5) (3×)	2.452	107.9			
	O(m4)	1.507						
	Si(3×)	3.118						

^a Values pertaining to every tetrahedral group are given in the order: distances from central P, tetrahedral edge lengths, and bond angles. The notation (*mn*) means that the value is a mean of *n* individual values, while (*n*×) means that the value occurs *n* times because of the symmetry at the central atom. Estimated standard deviations of the individual values are: P-O, 0.011 Å; O-O, 0.014 Å; O-P-O, 0.6°; P-Si, 0.006 Å; P-O-P, 0.7°.

TABLE VIII

MEAN VALUES OF INTERATOMIC DISTANCES AND BOND ANGLES IN SiP_2O_7 , AVERAGED OVER THE UNIT CELL^a

Interatomic distance (Å)		Bond angle (°)	
P-O(<i>m</i> 38)	1.524		
P-O _T (<i>m</i> 27)	1.506		
P-O _B (<i>m</i> 11)	1.577		
O _T -O _T (<i>m</i> 27)	2.490	O _T -P-O _T (<i>m</i> 27)	111.5
O _B -O _T (<i>m</i> 27)	2.482	O _B -P-O _T (<i>m</i> 27)	107.3
O-O(<i>m</i> 54)	2.486	O-P-O(<i>m</i> 54)	109.4
P-Si(<i>m</i> 27)	3.130	P-O-Si(<i>m</i> 27)	148.8
P-P(<i>m</i> 6)	3.027	P-O-P(<i>m</i> 6)	149.6
Si-O(<i>m</i> 27)	1.752		
O-O(<i>m</i> 54)	2.478	O-Si-O(<i>cm</i> 54)	90.0
O-O(<i>m</i> 14)	3.504	O-Si-O(<i>tm</i> 14)	177.8

^a The individual values from Tables VII and X were weighted according to their frequency within the unit cell. For further explanations, see footnotes to Tables VII and X.

of 1.752 Å in cubic SiP_2O_7 appears to be the shortest on record (24). The deviations of the individual O-O distances and of the O-Si-O angles from the values expected for an ideal octahedron are small but appear to be real. The individual Si-O bond lengths scatter appreciably (from 1.704 to 1.788 Å). This scatter is almost eight times the estimated standard deviation of the bond length and should, therefore, be real. Bissert and Liebau (15) observed a similar scatter in $\text{SiP}_2\text{O}_7\text{-AIII}$. They attempted to correlate it with the variation in the Si-O-P angle, but found the evidence for such dependence

to be inconclusive. We can confirm this: neither P-O, nor Si-O, nor the sum of P-O and Si-O show any pronounced dependence on the angle Si-O-P (Table IX). We tested also the dependence of P-O_B on the angle P-O-P. This dependence can explain 35% of the variation in the P-O_B bond length. However, this result depends critically on the interpretation of the straight P-O-P bridges. If we assumed these 180° angles to be the result of a space averaging (see above) then the actual P-O_B bond lengths must be longer than indicated in Table VII for P-O(5) and P-O(6): consequently, the correlation coefficient would be further reduced.

Cubic SiP_2O_7 proves to combine two unusual features. It has a few straight P-O-P angles, the way they are usually only found in high-temperature phases, and it has silicon in octahedral coordination against oxygen, which is commonly expected in high-pressure phases only. Liebau (24) has remarked on the tendency of silicon to assume six-coordination against a given ligand when the electronegativity of other elements present in the compound is high (examples: SiP_2O_7 , $\text{Si}(\text{OH})_6^{2-}$ in thaumasite). For SiP_2O_7 , the additional influence of charge balancing [Pauling's electrostatic valence rule (25)] has to be pointed out: if Si were not six-coordinated but instead four-coordinated, two of the seven oxygen atoms would be coordinated to one P atom only (sum of bond strengths, $p_{\text{O}} = 1.25$ v.u.), four would be coordinated to one Si and one P atom ($p_{\text{O}} = 2.25$ v.u.) and one would be bonded to two P atoms ($p_{\text{O}} = 2.50$ v.u.). Such a distribution of bond strengths obviously would be less balanced than the one observed in the actual structure, where $p_{\text{O}_B} = 2.50$ v.u. and

TABLE IX

RESULTS OF WEIGHTED REGRESSION ANALYSES ON DATA FROM SiP_2O_7 POLYMORPHS^a

Dependent variable	Independent variable	<i>a</i>	<i>b</i>	<i>r</i>	%	<i>N</i>
$\log[\sin(\bar{\alpha}/2)]$	$\log(\overline{\text{P-O}})$	0.11(2)	-1.08(11)	-0.87	76	30
(P-O)	* P-O-P	1.68(4)	-0.0007(2)	-0.59	35	15
(P-O)	* P-O-Si	1.58(4)	-0.0005(2)	-0.30	9	39
(Si-O)	* P-O-Si	1.91(6)	-0.0011(4)	-0.38	15	39
(P-O) + (Si-O)	* P-O-Si	3.83(12)	-0.0021(8)	-0.39	15	39

^a The average $\bar{\alpha}$ is taken over the three O_T-P-O_T or the three O_B-P-O_T angles in a tetrahedron. The intercept is *a*, while *b* is the slope of the regression equation; correlation coefficient, *r*; percent variation explained, %; number of pairs of values used, *N*. Data from cubic SiP_2O_7 and from $\text{SiP}_2\text{O}_7\text{-AIII}$ and $\text{SiP}_2\text{O}_7\text{-AIV}$ have been used.

TABLE X
 INTERATOMIC DISTANCES AND BOND ANGLES IN SILICATE OCTAHEDRA^a

	Distance (Å)	Bond angle (°)	Distance (Å)	Bond angle (°)	Distance (Å)	Bond angle (°)	Distance (Å)	Bond angle (°)	Distance (Å)	Bond angle (°)			
Si(1)	O(25)	1.704	P(7)	144.8	Si-O(m6)	1.750	Si(2)	O(15)	1.729	P(3)	166.4	Si-O(m6)	1.750
	O(14)	1.734	P(10)	137.7	O-O(m12)	2.475		O(31)	1.735	P(7)	141.0	O-O(m12)	2.475
	O(28)	1.750	P(6)	147.1	O-Si-O(sc)	Bond angle (°)		O(17)	1.750	P(3)	158.2	O-Si-O(sc)	88.2
	O(29)	1.754	P(5)	142.7	O-Si-O(c)	87.5°		O(23)	1.753	P(6)	144.6	O-Si-O(c)	92.6
	O(8)	1.770	P(1)	137.1	O-Si-O(tm3)	91.4		O(27)	1.759	P(8)	145.8	O-Si-O(tm3)	179.2
	O(10)	1.786	P(1)	140.8	Si-O-P(m6)	141.7		O(11)	1.774	P(2)	136.6	Si-O-P(m6)	148.8
Si(3)	O(7)	1.741	P(11)	148.8	Si-O(m6)	Distance (Å)		O(16)	1.715	P(3)	150.6	Si-O(m6)	Distance (Å)
	O(26)	1.743	P(7)	158.1	O-O(m12)	1.755		O(32)	1.741	P(8)	149.7	O-O(m12)	1.758
						2.481							2.485
	O(19)	1.744	P(4)	173.1	O-Si-O(sc)	Bond angle (°)		O(21)	1.757	P(9)	153.4	O-Si-O(sc)	87.1
	O(13)	1.746	P(2)	147.1	O-Si-O(c)	86.6°		O(9)	1.770	P(1)	146.2	O-Si-O(c)	92.7
	O(33)	1.775	P(8)	149.5	O-Si-O(tm3)	92.7		O(18)	1.774	P(4)	160.4	O-Si-O(tm3)	177.2
	O(24)	1.778	P(5)	143.0	Si-O-P(m6)	176.4		O(22)	1.788	P(5)	149.2	Si-O-P(m6)	151.6
						153.3							
Si(5)	O(20)(3×)	1.750	P(4)	149.6	O-Si-O(sc)	88.0°		O(12)(6×)	1.730	P(2)	146.0	O-Si-O(sc)	89.2
	O(30)(3×)	1.760	P(6)	150.5	O-Si-O(c)	92.6		O-O(m12)	2.446			O-Si-O(c)	90.8
	O(m6)	1.755			O-Si-O(tm3)	177.6						O-Si-O(tm3)	180.0
	O-O(m12)	2.482			Si-O-P(m6)	150.1							

^a Values pertaining to every octahedron are given in the order: distances from central Si, angles Si-O-P, mean Si-O, mean octahedral edge length, smallest cis-angle O-Si-O(sc), largest cis-angle (c), mean of trans-angle O-Si-O, and mean Si-O-P angle. Estimated standard deviations of the individual values are: Si-O, 0.011 Å; Si-O-P, 0.7°; O-O, 0.014 Å; O-Si-O, 0.6°. For further explanations see footnote to Table VII.

$p_{O_T} = 1.92$ v.u. for the six terminal oxygen atoms. It is conceivable that in the present case this is also a contributing factor to the formation of a six-coordination around silicon.

Note added in proof: Professor A. F. Wells was kind enough to point out to us that high-pressure SiP_2 [T. WADSTEN, *Acta Chem. Scand.* **21**, 1374 (1967)], which is of pyrite-type, is based on the same net as cubic SiP_2O_7 . Topologically speaking SiP_2O_7 can be derived from SiP_2 by introducing an oxygen atom along every Si-P and P-P link. Of course the dimensions have to be altered too since for SiP_2 the cell constant $a = 5.431 \text{ \AA}$, while the corresponding cell constant of SiP_2O_7 equals 7.473 \AA . Both SiP_2O_7 and the pyrite-type are based on the same net. We thank Professor Wells for his comments on the manuscript.

Acknowledgments

We thank Professor O. W. Flörke for the crystals of SiP_2O_7 , Dr. K. Abraham for the electron microprobe analysis, Dr. V. Gramlich for help with the X ray programming system at Karlsruhe, and the University Computing Centers at Bochum, Karlsruhe, and Illinois at Chicago for providing computer time. One of the authors (W. H. Baur) also thanks Professor H. Wondratschek for the hospitality extended to him during a visiting stay at the University of Karlsruhe.

References

1. W. H. BAUR, *Acta Crystallogr.* **19**, 909 (1965).
2. L. PAULING, *J. Chem. Soc. (London)*, 1461 (1948).
3. W. H. BAUR, *Amer. Mineral.* **57**, 709 (1972).
4. R. D. SHANNON AND C. T. PREWITT, *Acta Crystallogr. B* **25**, 925 (1969).
5. W. H. BAUR, *Trans. Amer. Crystallogr. Assoc.* **6**, 129 (1970).
6. W. H. BAUR, *Amer. Mineral.* **56**, 1573 (1971).
7. W. M. MEIER AND H. VILLIGER, *Z. Kristallogr.* **129**, 411 (1969).
8. W. H. BAUR, *Nature Phys. Sci.* **233**, 135 (1971).
9. V. GRAMLICH AND W. M. MEIER, *Z. Kristallogr.* **133**, 134 (1971).
10. G. R. LEVI AND G. PEYRONEL, *Z. Kristallogr.* **92**, 190 (1935).
11. H. VÖLLENKLE, A. WITTMANN, AND H. NOWOTNY, *Monatsh. Chem.* **94**, 956 (1963).
12. L.-O. HAGMAN AND P. KIERKEGAARD, *Acta Chem. Scand.* **23**, 327 (1969).
13. F. LIEBAU, G. BISSERT, AND N. KOPPEN, *Z. Anorg. Allg. Chem.* **359**, 113 (1968).
14. F. LIEBAU AND K.-F. HESSE, *Z. Kristallogr.* **133**, 213 (1971).
15. G. BISSERT AND F. LIEBAU, *Acta Crystallogr. B* **26**, 233 (1970).
16. W. H. BAUR AND A. A. KHAN, *Acta Crystallogr. B* **26**, 1584 (1970).
17. P. W. R. CORFIELD, R. J. DOEDENS, AND J. A. IBERS, *Inorg. Chem.* **6**, 197 (1967).
18. "International Tables for X-ray Crystallography," Vol. 3, p. 202, Kynoch Press, Birmingham, England, 1962.
19. L. KATZ AND H. D. MEGAW, *Acta Crystallogr.* **22**, 639 (1967).
20. B. E. ROBERTSON AND C. CALVO, *Can. J. Chem.* **46**, 605 (1968).
21. W. H. BAUR AND A. A. KHAN, *Acta Crystallogr. B* **27**, 2133 (1971).
22. A. F. WELLS, *Acta Crystallogr.* **18**, 894 (1965).
23. D. E. WILLIAMS, *Trans. Amer. Crystallogr. Assoc.* **6**, 21 (1970).
24. F. LIEBAU, *Bull. Soc. Fr. Min. Cristallogr.* **94**, 239 (1971).
25. L. PAULING, "The Nature of the Chemical Bond," 3rd ed., Chap. 13, Cornell Univ. Press, Ithaca, New York (1960).